Influence of cracking and shear connection deformation on the behaviour of steel-concrete composite beams

João Cardoso
joao.matos.cardoso@tecnico.ulisboa.pt

Técnico Lisboa, Portugal

September 2014

Abstract

The effect of the shear connection deformation and of the cracking of the concrete flange on the hogging region are relevant aspects on the global response of steel-concrete composite beams, particularly, in what regards stress redistribution from concrete to steel, longitudinal distribution of shear flow and beam deflection. A finite element model is herein presented to provide a reliable tool of analysis of composite beams with partial interaction, taking into account the concrete's non-linear behaviour under tension. The numerical results are compared with experimental data to prove the accuracy of the model in the non-linear analysis of composite beams.
Keywords: Steel-concrete composite beams, deformable shear connection, concrete cracking, finite element method, non-linear analysis

1. Introduction

Over the last few decades steel-concrete composite structures have been widely applied in building construction, being adopted as floor or wall elements, as well as in bridge construction. The good performance of this structural elements is justified by the ability of employing the best characteristics of each material to the function it is expected to fulfil. Moreover, the composite action is provided by means of locking devices or mechanical connectors which have proven to be reliable and of easy application. Steel and concrete have also a quite similar thermal expansion coefficient which renders their combination even more advantageous.

This work deals specifically with steel-concrete composite beams typically composed by a hot rolled I-beam or a plate girder together with a concrete flange. The two parts are connected to one another through mechanical connectors, being usually adopted headed studs.

The stiffness of a composite beam depends on its degree of interaction. When the shear connection is rigid enough to prevent slip, the interaction between both materials is total, otherwise it is classified as partial interaction. As for resistance, a composite beam is considered to have total connection whenever its ultimate limit state is not determined by the connection capacity. A composite beam is assumed to be in a state of partial connection if its resistance is limited by the shear connectors ultimate strength. Despite being intimately related, the degree of interaction and the degree of connection are quite different concepts dealing with different aspects of the composite beams' behaviour.

The problem of partial interaction and the cracking of the concrete flange on the hogging region of composite beams are the main objectives of this study. In fact, the flexibility of the shear connection plays a crucial role in the overall response of composite beams, particularly in what regards deflection, stress redistribution between the concrete slab and the steel beam and shear flow longitudinal distribution.

Since the middle of the last century, analytical and numerical models as well as experimental tests were carried out in order to better evaluate the composite beams behaviour. Some of these works as Newmark's [1], Aribert's [2] or Ansourian's [3] are worth being highlighted.

In 1951, Newmark *et al* [1] formulated the model which has served as basis to almost all the subsequent works dealing with the partial interaction problem. It consist of two Euler-Bernoulli beams coupled by means of a uniformly distributed spring

allowing only longitudinal relative displacements. Later on, Adekola [4] proposed a more general model taking into account the vertical relative displacement between the concrete slab and the steel beam, which was observed and measured in experimental tests made by Chapman and Balakrishnan [5] (cited by [2, 6]). Adekola has further suggested the model implementation through the finite difference method.

Derived from Newmark's formulation several analytical models, seeking closed-form solutions for the governing differential equations describing the partial interaction problem, have been proposed to evaluate the influence of the shear connection deformation [7, 8, 9].

Newmark's hypothesis of assimilating a composite beam to two Euler-Bernoulli beams bonded to one another through longitudinally deformable springs, has also been considered by several authors in order to develop numerical approximate solutions through the FEM theory. Several kinds of one-dimension finite elements were proposed in the last years.

In 1998, Salari *et al* [10] have compared the effectiveness between two different approaches, the approximation of internal forces or the approximation of displacements fields. Both were implemented in a non-linear analysis process, where the forces approximation have exhibited superior ability to perform. However, some difficulties arise in choosing the force interpolation functions. For a statically determinate element, the force interpolation functions resulting from the equilibrium correspond to the exact distribution of internal forces. The existence of a bond force at the interface renders the composite beam in a statically indeterminate element and therefore the choice of those interpolation functions is not trivial. Furthermore, the approximation of the forces field does not ensure local compatibility as well as the approximation of the displacements field does not ensure local equilibrium.

In order to overcome these limitations, in 2000, Ayoub and Filipou [11] developed a two-field mixed element, by approximating independently internal forces and displacement fields, which seems to combine the advantages of both formulations. In this model the two axial forces and the summation of the bending moments on each element were approximated by force interpolation functions whereas the bond force at the interface was described by the displacement field. This new approach was further extended by Dall'Asta and Zona [12], who formulated a three-field mixed finite element based on the approximation of displacements, strains and forces fields.

Some modifications to Newmark's kinematical model have been proposed by some authors studying the significance of shear strain, mainly on the steel beam element, in order to evaluate the global response of composite beams with deformable connection. In 2011, Zona and Ranzi [13] tested a new finite element model for physical non-linear analysis of composite beams in combined bending and shear. Firstly, they have assigned a Timoshenko beam only to the steel beam and then to both the concrete slab and the steel part. Through comparison with experimental results this model has proven to be a more suitable tool for short beams with small span-to-depth ratios and with higher levels of shear connection stiffness.

Lately, Nguyen *et al* [9] and Faella *et al* [14] presented an analytical solution of the governing equations describing the behaviour of a composite beam with deformable shear connection. By so doing, they have formulated an "exact" one-dimension finite element which may be implemented into the usual codes of finite elements analysing composite beams with partial interaction. The new model has exhibited the ability to orientate design in the linear range by utilising only one element per member of a continuous beam.

The model formulated in this work has adopted the Newmark's hypotheses and it was implemented through the finite element method by approximating the displacement field. The model was adopted to study the influence of the structural concrete's cracking and shear connection deformation on the overall response of composite beams. A Serviceability Limit State (SLS) analysis is performed for two different constitutive relations of concrete under tension by considering the strain-softening branch or by neglecting the concrete's resistance.

2. Analytical model

2.1. Basic assumptions

A steel-concrete composite beam is represented in figure 1, being adopted as reference an orthonormal system $\{O;\ X,\ Y,\ Z\}$. The beam is composed by two elements and occupies the spatial region $V = A \times L$, in which A represents its cross section and L the beam length. The composite cross section is formed by two parts with areas A_1 and A_2, corresponding to the concrete slab and to the steel girder, which for ease of notation are referred to as elements 1 and 2, respectively. The cross section is orthogonal to the X axis and symmetric about the bending plane XZ. z_c is the z coordinate of the interface between the two elements and $z_1,\ z_2$ are the respective z coordinates of the centroids of elements 1 and 2. The unit vectors corresponding to the axis $X,\ Y,\ Z$ are represented by **i, j, k**, respectively.

In spite of being obtained by a set of connectors with a discrete distribution, the connection between the two elements is assumed to be continuously distributed over the steel-concrete interface, without

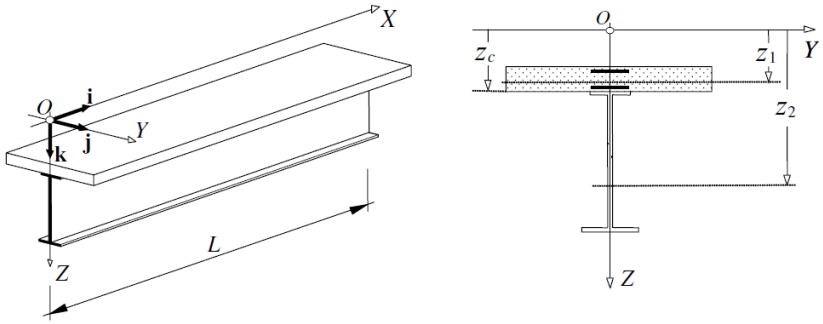

Figure 1: Composite beam and cross section (adapted from [6]).

any loss of validity [15, 10](cited by [16]). This connection provides composite behaviour, though it permits relative displacements in the longitudinal direction, which is known as slip.

Bernoulli's hypothesis is assumed to be valid for each element of the composite beam, that is, plane sections remain plane. No torsional or out-of-plane flexural effects are taken into account.

2.2. Compatibility conditions

Based on Newmark's derived model, the kinematical model adopted to describe the behaviour of the composite beam considers plane sections to remain plane except for a relative displacement at the connection interface. The variables of the corresponding displacement field are represented by the vector **d** as follows.

$$\mathbf{d}^T = \begin{bmatrix} u_1(x) & u_2(x) & w(x) \end{bmatrix}$$

where $u_1(x)$ and $u_2(x)$ represent the axial displacement at the centroid of elements 1 and 2, and $w(x)$ represent the vertical displacement of the composite beam. For ease of notation the displacements will be referred to as u_1, u_2, w. The displacement of an arbitrary point of the element α (with $\alpha = 1,\ 2$) can then be defined by the following vectors:

$$\mathbf{u}_\alpha(x,z) = w\mathbf{k} + [u_\alpha - (z - z_\alpha)\frac{dw}{dx}]\mathbf{i} \quad \text{on } A_\alpha, \forall x \in [0,L] \tag{1}$$

Since the small displacements hypothesis is considered to be valid, the non-null strain components are given by:

$$\varepsilon_\alpha(x,z) = \frac{\partial \mathbf{u}_\alpha(x,z)}{\partial x} \cdot \mathbf{i} = \frac{du_\alpha}{dx} - (z - z_\alpha)\frac{d^2w}{dx^2} \quad \text{on } A_\alpha, \forall x \in [0,L] \tag{2}$$

$$\chi(x) = -\frac{d^2w}{dx^2} \quad \forall x \in [0,L] \tag{3}$$

where $\varepsilon_\alpha(x,z)$ and $\chi_\alpha(x)$ are, respectively, the axial strain of the element α and the curvature of both elements.

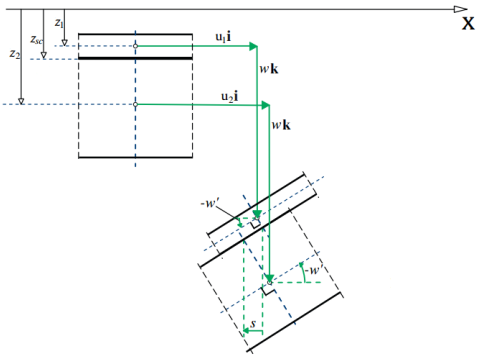

Figure 2: Kinematical model (adapted from [17])

For the complete kinematical description of the composite beam, relative displacements at the steel-concrete interface have also to be accounted for in the strain field. The adopted kinematical model is presented in figure 2.

The relative displacement at the connection interface is given by:

$$\delta(x) = \left(u_2 - u_1 - h\frac{dw}{dx}\right) \quad \forall x \in [0,L] \tag{4}$$

where $h = z_2 - z_1$, $z_{c1} = z_c - z_1$, $z_{c2} = z_c - z_2$, z_{c1} and z_{c2} can be positive or negative depending on the adopted reference system as shown in figure 1.

The strain field can be defined as a function of a deformation parameters vector whose components depend solely on the x coordinate of the section. These deformation parameters correspond to the axial strain at the fibres located at z_α, curvature and to the relative displacements at the connection interface.

$$\varepsilon_\alpha \equiv \varepsilon_\alpha(x, z_\alpha) = \frac{du_\alpha}{dx} \tag{5}$$

$$\chi \equiv \chi(x) \tag{6}$$

$$\delta \equiv \delta(x) \tag{7}$$

Thus, the strain field can be expressed by:

$$\boldsymbol{\varepsilon} = \mathbf{E}\,\mathbf{e} \tag{8}$$

in which $\boldsymbol{\varepsilon}$ is the strain field, $\mathbf{e}$ is the vector of the deformation parameters and $\mathbf{E}$ represents the deformation modes matrix.

$$\boldsymbol{\varepsilon}^T = \begin{bmatrix}\varepsilon_1(x,z) & \varepsilon_2(x,z) & \delta\end{bmatrix}$$

$$\mathbf{e}^T = \begin{bmatrix}\varepsilon_1 & \varepsilon_2 & \chi & \delta\end{bmatrix}$$

$$\mathbf{E} = \begin{bmatrix}1 & \cdot & z-z_1 & \cdot \\ \cdot & 1 & z-z_2 & \cdot \\ \cdot & \cdot & \cdot & 1\end{bmatrix}$$

The compatibility equations that define each deformation parameter can be rewritten in a matrix form as:

$$\mathbf{e} = \mathscr{D}\mathbf{d} \tag{9}$$

where $\mathbf{d}$ represents the displacement field, previously defined, and $\mathscr{D}$ is a compatibility differential operator defined as follows.

$$\mathscr{D} = \begin{bmatrix}\dfrac{d}{dx} & \cdot & \cdot \\ \cdot & \dfrac{d}{dx} & \cdot \\ \cdot & \cdot & -\dfrac{d^2}{dx^2} \\ -1 & 1 & h\dfrac{d}{dx}\end{bmatrix}$$

2.3. Equilibrium equations

A composite beam is assumed to be subjected to arbitrary axial and transverse uniformly distributed forces, p_{x1}, p_{x2}, p_z, and moments, m. The shear force, f is developed along the interface between the two elements.

Equilibrium differential equations established for both elements are given by:

$$\frac{dN_1}{dx} + p_{x1} + f = 0 \tag{10}$$

$$\frac{dV_1}{dx} + p_{z1} + f_z = 0 \tag{11}$$

$$\frac{dM_1}{dx} - V_1 + m_1 + z_{c1}f_x + f_\theta = 0 \tag{12}$$

$$\frac{dN_2}{dx} + p_{x2} - f_x = 0 \tag{13}$$

$$\frac{dV_2}{dx} + p_{z2} - f_z = 0 \tag{14}$$

$$\frac{dM_2}{dx} - V_2 + m_2 - z_{c2}f_x - f_\theta = 0 \tag{15}$$

where N_1, V_1, M_1, N_2, V_2 and M_2 represent the internal axial forces, shear forces and bending moments acting on the concrete and steel components, respectively. Because the shear deformation is neglected the shear force does not need to be explicitly considered in the equilibrium equations. By differentiating the sum of equations 12 and 15 and substituting equations 11 and 14 into the latter ones, it follows that:

$$\frac{d^2M}{dx^2} + p_z + \frac{dm}{dx} + h\frac{df_x}{dx} = 0 \tag{16}$$

where $M = M_1 + M_2$; $p_z = p_{z1} + p_{z2}$ and $m = m_1 + m_2$.

The resulting three equilibrium equations can be written in a compact form as follows.

$$\mathscr{D}^*\mathbf{s} - \mathscr{H}^*\mathbf{p} = \mathbf{0} \tag{17}$$

in which $\mathbf{s}$ and $\mathbf{p}$ are given by:

$$\mathbf{s}^T = \begin{bmatrix}N_1 & N_2 & M & f\end{bmatrix}$$

$$\mathbf{p}^T = \begin{bmatrix}p_{x1} & p_{x2} & p_z & m\end{bmatrix}$$

The equilibrium differential operator, $\mathscr{D}^*$, being self-adjoint[1] of $\mathscr{D}$ is defined as:

$$\mathscr{D}^* = \begin{bmatrix}\dfrac{d}{dx} & \cdot & \cdot & 1 \\ \cdot & \dfrac{d}{dx} & \cdot & -1 \\ \cdot & \cdot & \dfrac{d^2}{dx^2} & h\dfrac{d}{dx}\end{bmatrix}$$

$\mathscr{H}^*$ is self-adjointed to a differential operator $\mathscr{H}$ which is defined as:

$$\mathscr{H} = \begin{bmatrix}1 & \cdot & \cdot \\ \cdot & 1 & \cdot \\ \cdot & \cdot & 1 \\ \cdot & \cdot & -\dfrac{d}{dx}\end{bmatrix}$$

For the sake of the complete description of the problem eight boundary conditions must be specified.

$$u_\alpha(x) - \bar{u}_\alpha = 0 \quad on \quad \Gamma_u \tag{18a}$$

$$\frac{dw(x)}{dx} + \bar{\theta} = 0 \quad on \quad \Gamma_\theta \tag{18b}$$

$$w(x) - \bar{w} = 0 \quad on \quad \Gamma_w \tag{18c}$$

$$N_\alpha(x) - \bar{N}_\alpha = 0 \quad on \quad \Gamma_N \tag{18d}$$

[1] $d_{ij} = (-1)^{k+1} d^*_{ji}$

$$M(x) - \bar{M} = 0 \quad on \quad \Gamma_M \tag{18e}$$

$$\frac{dM(x)}{dx} + m + hf_x(x) - \bar{V} = 0 \quad on \quad \Gamma_V \tag{18f}$$

where Γ and the respective subscript denote the different kind of physical end conditions; $\bar{N}_\alpha$ is the concentrated horizontal load applied to the element α, and $\bar{V}$, $\bar{M}$ are the concentrated vertical load and bending moment applied to the composite beam.

2.4. Constitutive law

The constitutive laws for both materials can be compactly written by the following equation:

$$\boldsymbol{\sigma}^T = \boldsymbol{\varepsilon}^T \mathbf{C} = \begin{bmatrix} \sigma^1_{xx}(x,z) & \sigma^2_{xx}(x,z) & f \end{bmatrix} \tag{19}$$

where $\boldsymbol{\sigma}$ represents the stress field in the concrete slab and steel girder, corresponding, respectively, to elements 1 and 2; and the shear flow, f, at the steel-concrete interface. The strain field, $\boldsymbol{\varepsilon}$, is presented in equation 8.

The matrix $\mathbf{C}$, which relates the stress and strain fields, is formed by the Young's moduli associated with each element of the composite cross section and by the shear connection stiffness.

$$\mathbf{C} = \begin{bmatrix} E_1 & \cdot & \cdot \\ \cdot & E_2 & \cdot \\ \cdot & \cdot & k_c \end{bmatrix}$$

The constitutive law, given by equation 19, establishes a relation between continuous variables, namely the stress field and the strain field. However, a similar relation between the internal forces and the corresponding deformations located at an arbitrary section of the beam is also required.

From the linear theory of elasticity one knows that the elastic potential energy produced by the internal forces associated with a particular strain field must be equivalent to the potential energy produced by the corresponding stress field. This equivalence is stated in the following form:

$$\begin{aligned} \mathbf{s}^T \mathbf{e} &= \int_A \boldsymbol{\sigma}^T \boldsymbol{\varepsilon} \; dA \\ &\Leftrightarrow \mathbf{s} = \begin{bmatrix} \int_A \mathbf{E}^T \mathbf{C} \mathbf{E} \; dA & \cdot \\ \cdot & k_c \end{bmatrix} \mathbf{e} = \mathbf{K}\mathbf{e} \end{aligned} \tag{20}$$

being $\mathbf{s}$ the vector of the internal forces, $\mathbf{e}$ the vector of the deformations parameters and $\mathbf{E}$ the deformation modes matrix, accounting for the steel and concrete parts and excluding the connection interface.

The cross-sectional stiffness matrix of the two materials follows from equation 20:

$$\begin{aligned} \mathbf{K} &= \begin{bmatrix} \int_A \mathbf{E}^T \mathbf{C} \mathbf{E} \; dA & \cdot \\ \cdot & k_c \end{bmatrix} \\ &= \begin{bmatrix} E_1 A_1 & \cdot & E_1 S_1 & \cdot \\ \cdot & E_2 A_2 & E_2 S_2 & \cdot \\ E_1 S_1 & E_2 S_2 & EI_0 & \cdot \\ \cdot & \cdot & \cdot & k_c \end{bmatrix} \end{aligned}$$

with $EI_0 = E_1 I_1 + E_2 I_2$. A_α, S_α, I_α are, respectively, the cross-sectional area, first and second moments of area.

2.5. Analytical solution

Equations 10 to 15 were formerly written in terms of equilibrium. By substituting the compatibility conditions 9 and the constitutive laws 20 into the equation 17, equilibrium equations are obtained as functions of displacements.

$$\mathscr{D}_s^* \mathbf{K}_s \mathscr{D}_s \mathbf{d}_s - \mathscr{H}^* \mathbf{p}_s = \mathbf{0} \tag{21}$$

The development of the equation 21 yields the following equilibrium differential equations:

$$E_1 A_1 \frac{d^2 u_1}{dx^2} + k_c \left(u_2 - u_1 + h \frac{dw}{dx} \right) = -p_{x1} \tag{22a}$$

$$E_2 A_2 \frac{d^2 u_2}{dx^2} - k_c \left(u_2 - u_1 + h \frac{dw}{dx} \right) = -p_{x2} \tag{22b}$$

$$-EI_0 \frac{d^4 w}{dx^4} + hk_c \left(\frac{du_2}{dx} - \frac{du_1}{dx} + h \frac{d^2 w}{dx^2} \right) = -p_z - \frac{dm}{dx} \tag{22c}$$

Taking into account only the homogenised form of equations 22, i.e. not considering span loads, they can be stated in terms of the concrete axial displacement.

$$u_1^{\mathrm{v}} - \alpha^2 u''' = 0 \tag{23}$$

in which the primes and Roman numerals denote the derivative order with respect to the x coordinate and the constant α is function of mechanical and geometrical cross-sectional properties, being defined as:

$$\alpha^2 = k_c \left(\frac{EA_1 + EA_2}{E_1 A_1 E_2 A_2} + \frac{h^2}{EI_0} \right)$$

3. Numerical model

3.1. Finite element formulation

The displacement field, $\mathbf{d}$, at an element level, is approximated by a linear combination of interpolation functions.

$$\mathbf{d} \cong \boldsymbol{\Psi} \mathbf{q}_e \tag{24}$$

where $\mathbf{q}_e$ is the nodal displacements vector, which represents the weights (or amplitudes) of the approximation functions and $\mathbf{\Psi}$ is the matrix containing the approximation functions.

By substituting the approximation of the displacement field into equation 21 a residual is obtained. To ensure the equilibrium in a global sense, the residual is enforced to be null in a weighted sense over the element domain.

$$\int_0^{L_e} (\mathscr{D}\mathbf{\Psi})^T \mathbf{K} \mathscr{D}\mathbf{\Psi}\mathbf{q}_e \, dx = \int_0^{L_e} (\mathscr{H}\mathbf{\Psi})^T \mathbf{p} \, dx + [(\mathscr{H}\mathbf{\Psi})^T \mathbf{Q}]_{x=0,L_e} \quad (25)$$

where $\mathbf{Q}$ represents the vector of the concentrated loads applied at the ends of the element, being defined as follows:

$$\mathbf{Q}^T = \begin{bmatrix} \bar{N}_1 & \bar{N}_2 & \bar{V} & \bar{M} \end{bmatrix}$$

Equation 25 can be compactly written as follows:

$$\mathbf{K}_e \mathbf{q}_e = \mathbf{Q}_e \quad (26)$$

which corresponds to the well known equation of the displacement method, being $\mathbf{K}_e$ the stiffness matrix of the element.

$$\mathbf{K}_e = \int_0^{L_e} \mathbf{B}^T \mathbf{K}_s \mathbf{B} \, dx \quad (27)$$

where the matrix $\mathbf{B}$ is given by:

$$\mathbf{B} = \mathscr{D}_s \mathbf{\Psi}$$

The vector $\mathbf{Q}_e$ comprises both terms of the right-hand side of equation 25. The first term corresponds to the statically equivalent nodal forces,i.e., fictitious forces that associated with an arbitrary deformed shape of structure, produce the same work as the real load distributed along the element; the second term constitutes the concentrated loads applied at the boundary of the element.

$$\mathbf{Q}_e = \int_0^{L_e} (\mathscr{H}\mathbf{\Psi})^T \mathbf{p} \, dx + [(\mathscr{H}\mathbf{\Psi})^T \mathbf{Q}_s]_{x=0,L_e} \quad (28)$$

The finite element formulated in this section is locally compatible, that is, all compatibility conditions are verified at a local level along the element domain. On the other hand, the equilibrium is verified globally by equation 25, i.e., by weighting the interpolation functions [18]. It is worth mentioning that being a bar element and taking into account that the nodal displacement are exact, the nodal equilibrium is ensured.

3.2. Computer implementation

The numerical model proposed for the analysis of composite beams with flexible connection does not take into account the shear deformation on both the concrete and the steel components. The vertical and rotational deformations at the interface connection are also neglected.

The displacement-based finite element considered in the model implementation has 10 degrees of freedom, as depicted in figure 3, and approximates the axial and the vertical displacement fields by second and third order polynomials, respectively. Two additional internal nodes with axial freedom (u_{1m} and u_{2m}) are required for the second order polynomials.

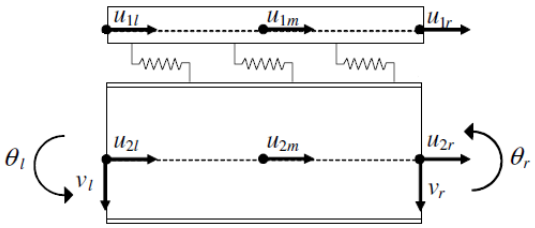

Figure 3: Locking-free 10dof element (adapted from [6]).

The nodal displacements vector $\mathbf{q}_e$ which represents the weights of the interpolations functions and the matrix $\mathbf{\Psi}$ storing the interpolation functions are given by:

$$\mathbf{q}_e^T = \begin{bmatrix} u_{1l} & u_{2l} & w_l & \theta_l & u_{1r} & u_{2r} & w_r & \theta_r & u_{1m} & u_{2m} \end{bmatrix}$$

$$\mathbf{\Psi} = \begin{bmatrix} \mu_l & \cdot & \cdot & \cdot & \mu_r & \cdot & \cdot & \cdot & \mu_m & \cdot \\ \cdot & \mu_l & \cdot & \cdot & \cdot & \mu_r & \cdot & \cdot & \cdot & \mu_m \\ \cdot & \cdot & \eta_l & \nu_l & \cdot & \cdot & \eta_r & \nu_r & \cdot & \cdot \end{bmatrix}$$

The quadratic polynomials adopted to approximate the longitudinal displacement field are defined as follows:

$$\mu_l = \frac{1}{2}\xi(\xi - 1) \quad (29a)$$

$$\mu_r = \frac{1}{2}\xi(\xi + 1) \quad (29b)$$

$$\mu_m = 1 - \xi^2 \quad (29c)$$

The Hermitian polynomials adopted to approximate the deflection field for an element are given by:

$$\eta_l = 1 - \frac{1}{4}(\xi + 1)^2(2 - \xi) \quad (30a)$$

$$\eta_r = \frac{1}{4}(\xi+1)^2(2-\xi) \tag{30b}$$

$$\nu_l = -\frac{1}{8}L_e(\xi+1)(1-\xi)^2 \tag{30c}$$

$$\nu_r = \frac{1}{8}L_e(\xi+1)^2(1-\xi) \tag{30d}$$

where $\xi = \frac{2x}{Le} - 1$ represents the natural coordinate utilised to apply the *Gauss-Lobatto quadrature* and L_e represents the element length.

4. Numerical examples

4.1. Introduction

The numerical solutions obtained through the developed program are compared with the analytical solutions, defined in section 2.5, to evaluate the effectiveness of the finite element formulated. To this end, a continuous beam of two equal spans subjected to a uniformly distributed load has been considered. This beam is 12 m long and its cross section is formed by a concrete slab of class C30/37 and dimension 3000 mm x 150 mm, and by a hot rolled steel beam IPE500 of grade S275.

In order to evaluate the influence of the connection stiffness in composite beams' behaviour, four different solutions were adopted . Two rows of connectors with 19 mm of diameter and a length of 100 mm were considered to be uniformly distributed with longitudinal spacings of 7000 mm, 1150 mm, 285 mm and 70 mm.

According to the shear connectors' constitutive law proposed by Johnson [19](cited by [16, 20, 15]) based on experimental results, a ρ modulus (relating shear force and displacement) of 150 kN/mm has been adopted. This value derives from the secant stiffness corresponding to 50% of the ultimate load a shear connector.

In 1993, Girhammar [21] introduced a dimensionless parameter αL representing the composite action, where L is the beam length and α is given by:

$$\alpha^2 = \rho_x \left(\frac{EA_0}{E_1 A_1 E_2 A_2} + \frac{h^2}{EI_0} \right)$$

For a single row of shear connectors with 19 mm of diameter and a length of 100 mm with a longitudinal spacing of 150 mm, an approximate secant stiffness of 10^6 kN/m^2 is estimated. Rendering this value into the Girhammar's stiffness parameter for a 12 m long beam it corresponds to $\alpha L = 14.8$, which is consistent with the ranges proposed by Girhammar [21], $1 < \alpha L < 15$ and Ranzi [6], $1 < \alpha L < 20$.

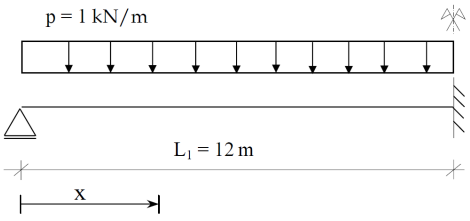

Figure 4: Continuous beam with two equal spans (model with symmetry simplification) subjected to a uniform distributed load.

A parametric study is herein performed for values of $\alpha L = 2,\ 5,\ 10$ and 20 (which correspond respectively to the longitudinal spacings of 7000 mm, 1150 mm, 285 mm and 70 mm) to investigate the influence of the shear connection stiffness on the overall structural response.

4.2. Linear analysis of a two-spam continuous beam

A two-span continuous beam subjected to a unitary distributed load, as represented in figure 4.

Through the analysis of figure 5 representing the analytical solution of vertical displacements, one concludes that by enhancing the connection flexibility greater deflections are obtained. In fact, the mid-span deflection corresponding to the highest connection stiffness value ($\alpha L = 20$) is less than 50% of the mid-span deflection obtained for the lowest connection stiffness ($\alpha L = 2$). The comparison between analytical and numerical solutions presented in figure 6 proves, once more, the reliability of this finite element model to evaluate displacements.

The longitudinal distribution of shear flow over the steel-concrete interface is represented in figure 7. The end support and the hogging regions are those where the influence of the connection stiffness is evident. The variation of shear flow along the beam length is flattened as the connection stiffness decreases. Figure 8 reveals a large error when a mesh with a single element is utilised to evaluate the shear flow at the end support section. However the high convergence rate of this method renders

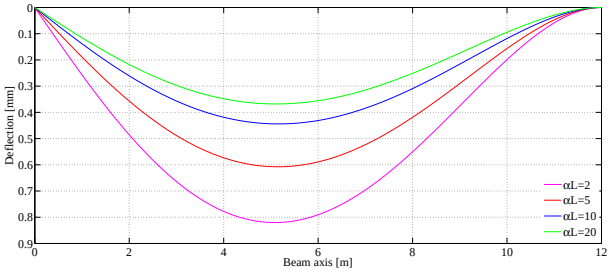

Figure 5: Vertical displacement of the composite beam (analytical solution).

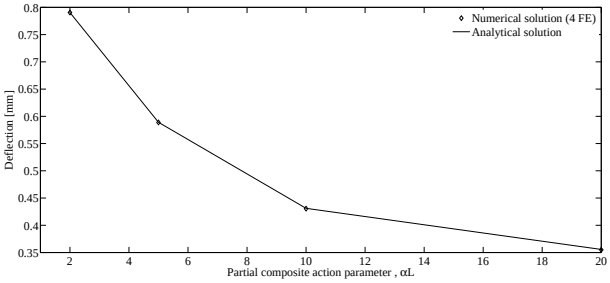

Figure 6: Mid-span deflection of the composite beam (numerical solution/analytical solution).

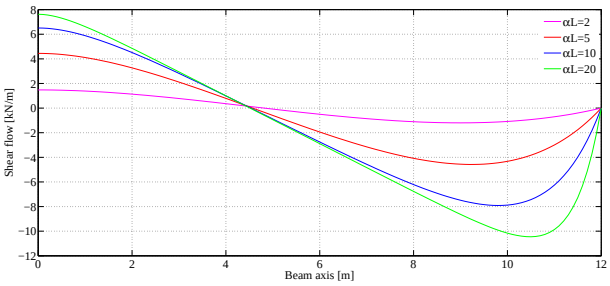

Figure 7: Shear flow distribution along the steel-concrete interface (analytical solution).

the error acceptable when four finite elements are used in this approximation.

The numerical model with a uniform four-element mesh provides reliable results in what concerns the longitudinal distribution of the axial stress of the concrete slab's top and bottom fibres. The good agreement between numerical and analytical solutions can be seen in figure 9.

A comparison between the numerical solution, considering four finite elements, and the analytical solution of the longitudinal distribution of the shear flow at the connection interface is plotted in figure 10. As shown in the example of a concentrated load acting on a simply supported composite beam, the numerical solution does not perform a good approximation for higher values of the connection stiffness

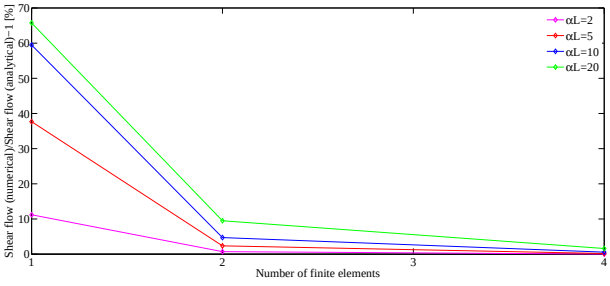

Figure 8: Error in the approximation of the shear flow at the end support section of the composite beam (numerical solution/analytical solution).

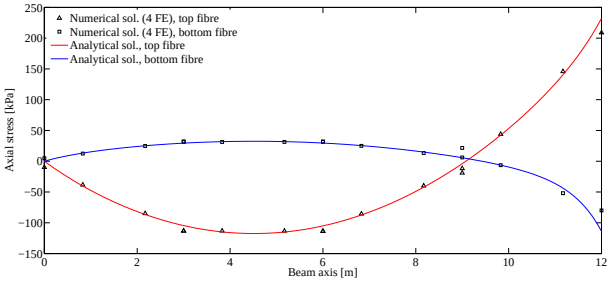

Figure 9: Axial stress in the concrete slab.

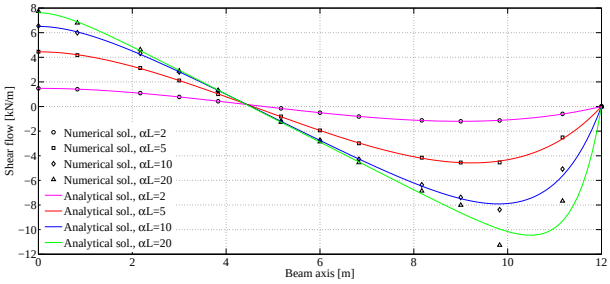

Figure 10: Shear flow distribution along the steel-concrete interface (numerical solution with 4 FE/analytical solution).

on the hogging region, where the shear flow gradient is significant.

5. Comparison with experimental data

The non-linear model was adopted to evaluate the influence of concrete's cracking and shear connection deformation on the structural behaviour of composite beams. To be used as a reliable tool of analysis the model's accuracy is verified by comparing its results with experimental data. In this section, four different beams are considered, two simply-supported beams and two continuous beams with two spans.

It is worth mentioning that the numerical model developed in this work remains valid only for the structural steel linear range, since no plasticity was considered for steel's constitutive law.

5.1. Simply supported beams

Two simply supported beams corresponding to those tested by Chapman and Balakrishnan [5] were analysed using the proposed numerical model. Both beams have a 5.490 m long span, a hot rolled I-shaped steel beam 12"×6"×44 lb/ft BSB (British Standard Beam) and a concrete slab 0.152 m thick and 1.220 m wide, as represented in figure 11). Beam E1 is subjected to a midspan concentrated load, whereas beam U4 is subjected to a uniformly distributed loading. Shear connectors were disposed according to shear flow elastic longitudinal distribution. Thus, two rows of headed studs with 12.7 mm of diameter and 50 mm height are equally

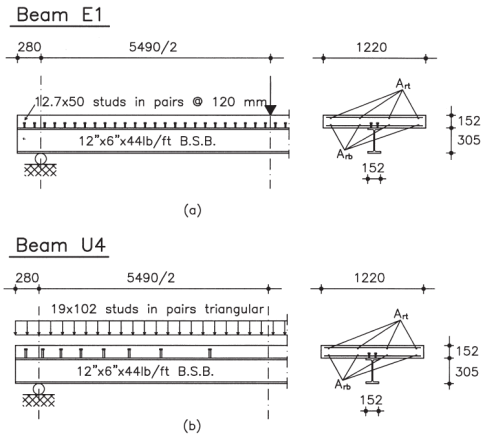

Figure 11: Geometrical properties of simply supported beams (adapted from [22, 5]).

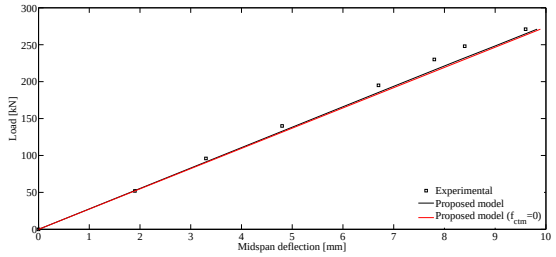

Figure 12: Comparison between experimental and numerical results of load-deflection curve for beam E1.

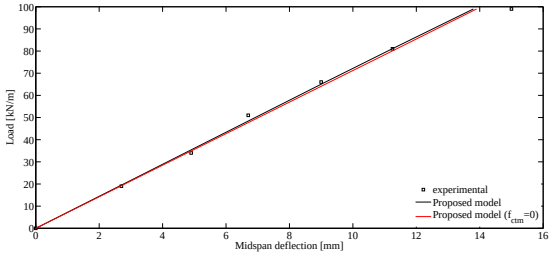

Figure 13: Comparison between experimental and numerical results of load-deflection curve for beam U4.

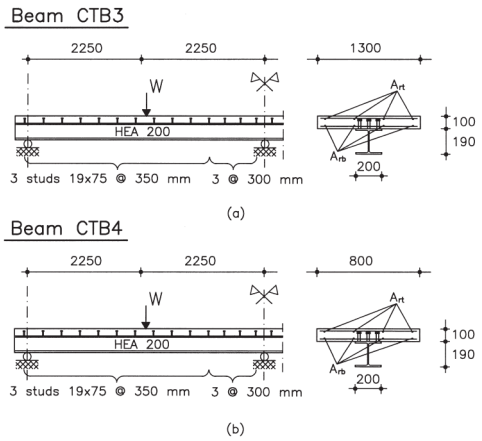

Figure 14: Geometrical properties of continuous beams (adapted from [22, 5]).

distributed at 120 mm along beam E1's length, whereas beam U4 has headed studs with 19 mm of diameter and 102 mm height linearly distributed over its interface connection.

Because both beams allow symmetry simplifications, meshes with four elements per half span were adopted in numerical tests. Shear connectors were assumed to be uniformly distributed along each finite element's length.

A comparison between experimental and numerical results for load versus midspan deflection curves for beams E1 and U4 is represented in figures 12 and 13. It can be observed the good agreement between experimental and numerical results. The small discrepancies are possibly due to the contact bond acting at the steel-concrete interface which was neglected [22, 5].

5.2. Two-span continuous beams

Beams CTB3 and CTB4, tested by Ansourian [3], were considered in order to verify the numerical model's accuracy on the hogging region. Both beams are represented in figure 14.

Either beam CTB3 or beam CTB4 have two equal spans of 4.5 m, a hot rolled H-shaped steel beam HEA 200 and three rows of headed stud connectors with 19 mm of diameter and 75 mm height equally spaced at 350 mm over the beam except over the hogging region, 1.050 m for both sides of the internal support, where the spacing between connectors decrease to 300 mm. Beam CTB3's concrete slab has a thickness of 0.100 m and a breadth of 1.300 m, whereas beam CTB4 possesses one with 0.100 m of thickness and 0.800 m of breadth. Either beam CTB3 or beam CTB4 are loaded with symmetrical midspan concentrated loads.

Again, symmetry simplifications are applied in order to gain computational efficiency, and meshes of four elements per span are employed.

The experimental and numerical results of deflection and curvature at midspan and curvature at the internal support varying with the load acting on beam CTB3 are represented in figures 15 and 16. It should be mentioned that the hogging curvature was not measured right at the support section but at 150 mm from it [22, 8]. It can be noticed that both curves, experimental and numerical, are very close, mainly in what regards load versus deflection and load versus support curvature, which certify the reliability of the proposed model.

A comparison between experimental and numerical results for beam CTB4, namely the curves of

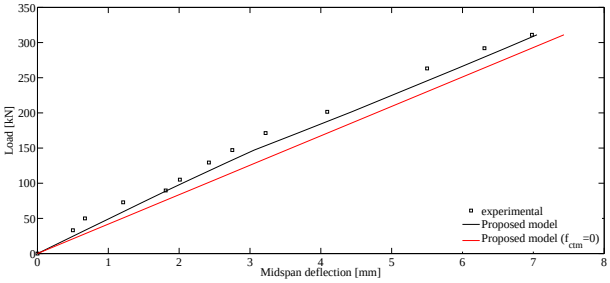

Figure 15: Comparison between experimental and numerical results of load-deflection curve for beam CTB3.

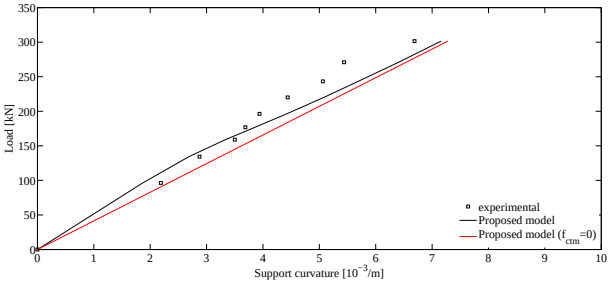

Figure 16: Comparison between experimental and numerical results of load versus support curvature curve for beam CTB3.

load versus midspan deflection and load versus support curvature, is presented in figures17 and 18, respectively. The hogging curvature was also measured at 150 mm from the internal support. Again, experimental and numerical curves are in a good agreement, confirming the ability of the proposed model to study the influence of structural concrete's cracking and of connection deformation in composite beams global response.

6. Conclusions

In this paper, the influence in the global response of composite beam of both the shear connection deformation and the cracking of the concrete flange over the hogging region was investigated.

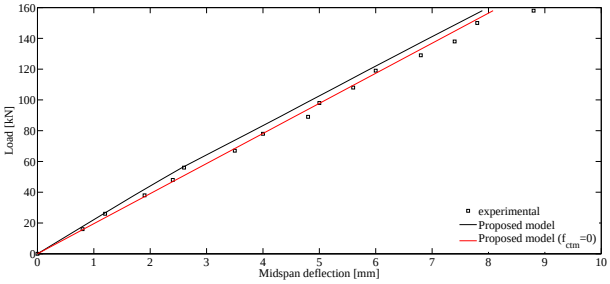

Figure 17: Comparison between experimental and numerical results of load-deflection curve for beam CTB4.

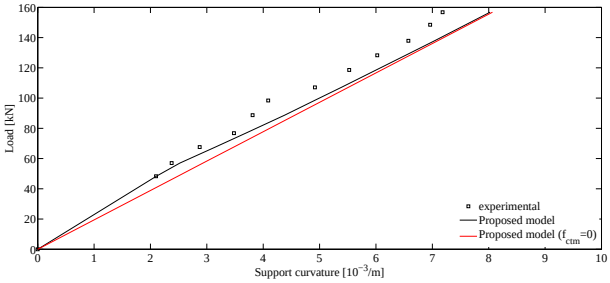

Figure 18: Comparison between experimental and numerical results of load versus support curvature curve for beam CTB4.

An analytical model, based on Newmark's hypotheses, formulated. The system of differential equations governing the problem of partial interaction in composite beams is solved and a parametric study concerning the shear connection stiffness is performed.

A finite element approximating the displacements field is formulated in order to provide a reliable tool to evaluate the stress redistribution between the concrete slab and the steel beam induced by the connection deformation and concrete's cracking.

A non-linear constitutive law for concrete under tension is adopted and the algorithm underlying its implementation, the so-called Newton-Raphson method, is explained.

It was concluded that a higher shear connection stiffness, i.e., a larger composite action between steel and concrete, results in lower displacements. Thus, constraining the longitudinal slip between steel and concrete significantly contributes to reduce vertical displacements of composite beams. In the hogging region, the cracking of the concrete flange causes a redistribution of stress from concrete to steel, increasing the flexibility of the composite beam. The tension stiffening effect has proved to be not negligible for a limited load range.

Experimental tests available in literature were used as benchmark in order to validate the finite element model proposed. The good agreement between numerical and experimental results proves the ability of this method to study composite beams with partial interaction even when accounting for concrete's non-linear behaviour over the hogging region.

References

[1] Nathan M Newmark, Chester P Siess, and IvanM Viest. Tests and analysis of composite beams with incomplete interaction. *Proc Soc Exp Stress Anal*, 9(1):75–92, 1951.

[2] JM Aribert and K Abdel Aziz. Calcul des poutres mixtes jusqu'à l'état ultime avec un

effet de soulèvement à l'interface acier-béton. *CONSTR MET*, (4), 1985.

[3] P Ansourian. Experiments on continuous composite beams. In *ICE Proceedings*, volume 73, pages 26–51. Thomas Telford, 1982.

[4] AO Adekola. Partial interaction between elastically connected elements of a composite beam. *International Journal of Solids and Structures*, 4(11):1125–1135, 1968.

[5] JC Chapman and S Balakrishnan. Experiments on composite beams. *The Structural Engineer*, 42(11):369–383, 1964.

[6] G Ranzi, F Gara, and P Ansourian. General method of analysis for composite beams with longitudinal and transverse partial interaction. *Computers & structures*, 84(31):2373–2384, 2006.

[7] Ulf Arne Girhammar and Vijaya KA Gopu. Composite beam-columns with interlayer slip-exact analysis. *Journal of Structural Engineering*, 119(4):1265–1282, 1993.

[8] HY Loh, B Uy, and MA Bradford. The effects of partial shear connection in the hogging moment regions of composite beams part iianalytical study. *Journal of Constructional Steel Research*, 60(6):921–962, 2004.

[9] Quang-Huy Nguyen, Enzo Martinelli, and Mohammed Hjiaj. Derivation of the exact stiffness matrix for a two-layer timoshenko beam element with partial interaction. *Engineering Structures*, 33(2):298–307, 2011.

[10] M Reza Salari, Enrico Spacone, P Benson Shing, and Dan M Frangopol. Nonlinear analysis of composite beams with deformable shear connectors. *Journal of Structural Engineering*, 124(10):1148–1158, 1998.

[11] Ashraf Ayoub and Filip C Filippou. Mixed formulation of nonlinear steel-concrete composite beam element. *Journal of Structural Engineering*, 126(3):371–381, 2000.

[12] Andrea Dall'Asta and Alessandro Zona. Three-field mixed formulation for the non-linear analysis of composite beams with deformable shear connection. *Finite Elements in Analysis and Design*, 40(4):425–448, 2004.

[13] Alessandro Zona and Gianluca Ranzi. Finite element models for nonlinear analysis of steel–concrete composite beams with partial interaction in combined bending and shear. *Finite Elements in Analysis and Design*, 47(2):98–118, 2011.

[14] Ciro Faella, Enzo Martinelli, and Emidio Nigro. Steel–concrete composite beams in partial interaction: Closed-form exact expression of the stiffness matrix and the vector of equivalent nodal forces. *Engineering Structures*, 32(9):2744–2754, 2010.

[15] JM Aribert, E Ragneau, and H Xu. Développement dun élément fini de poutre mixte acier-béton intégrant les phénomènes de glissement et de semi-continuité avec éventuellement voilement local. *Revue Construction Métallique*, 2:31–49, 1993 [in French].

[16] Ricardo Vieira. Anlise de vigas mistas: influncia da deformabilidade da conexo e dos efeitos diferidos. Master's thesis, Instituto Superior Tcnico, Universidade Tcnica de Lisboa, 2000 [in Portuguese].

[17] Andrea DallAsta and Alessandro Zona. Nonlinear analysis of composite beams by a displacement approach. *Computers & structures*, 80(27):2217–2228, 2002.

[18] Jacob Fish and Ted Belytschko. *A first course in finite elements*. John Wiley and Sons, 2007.

[19] RP Johnson, N Molenstra, et al. Partial shear connection in composite beams for buildings. In *ICE Proceedings*, volume 91, pages 679–704. Thomas Telford, 1991.

[20] Luís Calado and João Santos. Estruturas mistas de aço e betão. 2009.

[21] Ulf Arne Girhammar and Danhua Pan. Dynamic analysis of composite members with interlayer slip. *International journal of solids and structures*, 30(6):797–823, 1993.

[22] N Gattesco. Analytical modeling of nonlinear behavior of composite beams with deformable connection. *Journal of Constructional Steel Research*, 52(2):195–218, 1999.